

USAARL Report No. 96-13



Figures of Merit and Performance Specifications for the IHADSS and ANVIS

By

Thomas H. Harding
John S. Martin
Howard H. Beasley

UES, Inc.
Dayton, OH

and

Clarence E. Rash

Aircrew Health and Performance Division

February 1996

Approved for public release; distribution unlimited.

U.S. Army Aeromedical Research Laboratory
Fort Rucker, Alabama 36362-0577

Notice

Qualified requesters

Qualified requesters may obtain copies from the Defense Technical Information Center (DTIC), Cameron Station, Alexandria, Virginia 22314. Orders will be expedited if placed through the librarian or other person designated to request documents from DTIC.

Change of address

Organizations receiving reports from the U.S. Army Aeromedical Research Laboratory on automatic mailing lists should confirm correct address when corresponding about laboratory reports.

Disposition

Destroy this document when it is no longer needed. Do not return it to the originator.

Disclaimer

The views, opinions, and/or findings contained in this report are those of the author(s) and should not be construed as an official Department of the Army position, policy, or decision, unless so designated by other official documentation. Citation of trade names in this report does not constitute an official Department of the Army endorsement or approval of the use of such commercial items.

Reviewed:



RICHARD R. LEVINE

LTC, MS

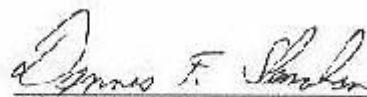
Director, Aircrew Health and
Performance Division



ROGER W. WILEY, O.D., Ph.D.

Chairman, Scientific
Review Committee

Released for publication:



DENNIS F. SHANAHAN

Colonel, MC, MFS
Commanding

Unclassified

SECURITY CLASSIFICATION OF THIS PAGE

REPORT DOCUMENTATION PAGE				Form Approved OMB No. 0704-0188	
1a. REPORT SECURITY CLASSIFICATION Unclassified			1b. RESTRICTIVE MARKINGS		
2a. SECURITY CLASSIFICATION AUTHORITY			2. DISTRIBUTION/AVAILABILITY OF REPORT Approved for public release; distribution unlimited		
2b. DECLASSIFICATION/DOWNGRADING SCHEDULE					
4a. PERFORMING ORGANIZATION REPORT NUMBER(S) USAAFL Report No. 96-13			5. MONITORING ORGANIZATION REPORT NUMBER(S)		
5a. NAME OF PERFORMING ORGANIZATION U.S. Army Aeromedical Research Laboratory		5b. OFFICE SYMBOL (If applicable) MCMR-UAS-VS	7a. NAME OF MONITORING ORGANIZATION U. S. Army Medical Research and Material Command		
6a. ADDRESS (City, State, and ZIP Code) P.O. Box 620577 Fort Rucker, AL 36362-0577			7b. ADDRESS (City, State, and ZIP Code) Fort Detrick Frederick, MD 27102-5012		
8a. NAME OF FUNDING/SPONSORING ORGANIZATION		8b. OFFICE SYMBOL (If applicable)	9. PROCUREMENT INSTRUMENTS IDENTIFICATION NUMBER		
8c. ADDRESS (City, State, and ZIP Code)			10. SOURCE OF FUNDING NUMBERS		
			PROGRAM ELEMENT NO. 0602787A	PROJECT NO. 787A879	TASK NO. PE
					WORK UNIT ACCESSION NO. 164
11. TITLE (Include Security Classification) (U) Figures of Merit and Performance Specifications for the IHADSS and ANVIS					
12. PERSONAL AUTHOR(S) Thomas H. Harding, Howard H. Beasley, John S. Martin, Clarence E. Rash					
13a. TYPE OF REPORT Final		13b. TIME COVERED FROM _____ TO _____		14. DATE OF REPORT (Year, Month, Day) 1996 January	
15. SUPPLEMENTARY NOTATION					
17. GOSAT CODES			18. SUBJECT TERMS (Continue on reverse if necessary and identify by block number)		
FIELD	GROUP	SUB-GROUP			
20	05				
06	05		AH-64, helmet display unit, testing and evaluation, optical performance		
19. ABSTRACT (Continue on reverse if necessary and identify by block number)					
<p>The U.S. Army currently fields two helmet mounted display systems. These are the Integrated Helmet and Display Sighting System (IHADSS), which is employed on the AH-64 Apache, and the Aviator's Night Vision Imaging System (ANVIS), which is employed on all U.S. Army rotary wing aircraft. The performance and figures-of-merit specifications provide the basis for judging performance of future aviation electro-optical devices. This paper specifies in summary form performance parameters for different figures-of-merit which can be used to define the overall performance of the IHADSS and ANVIS.</p>					
20. DISTRIBUTION/AVAILABILITY OF ABSTRACT <input checked="" type="checkbox"/> UNCLASSIFIED/UNLIMITED <input type="checkbox"/> SAME AS RPT. <input type="checkbox"/> DTIC USERS			21. ABSTRACT SECURITY CLASSIFICATION Unclassified		
22a. NAME OF RESPONSIBLE INDIVIDUAL Chief, Scientific Information Center			22b. TELEPHONE (Include Area Code) 534-255-6907		22c. OFFICE SYMBOL MRMC-UAX-SI

Table of contents

List of figures	4
List of tables	4
Introduction	5
IHADSS specifications	5
IHADSS optical specifications	6
Combiner lens transmittance	6
Distortion	6
Optical aberrations	7
Magnification	7
Field-of-view	9
Eye relief	9
Exit pupil	9
Focus adjustment range	9
IHADSS electro-optical specifications	9
Dynamic luminance range	9
Dynamic modulation transfer function (MTF)	9
Contrast ratios	10
Gray shades	10
Display chromaticity	11

Table of contents (Cont)

Display uniformity	11
Visual performance with the IHADSS	11
Resolution and ambient light levels	11
Field-of-view	11
ANVIS specifications	11
ANVIS optical specifications	12
Distortion	12
Magnification	12
Eyere relief	13
Exit pupil	13
Focus adjustment range	13
Interpupillary adjustment	13
Collimation	13
ANVIS electro-optical specifications	13
Dynamic luminance range	13
Dynamic MTF	14
Gray shades	14
Contrast ratio	14
Gain	14
Display chromaticity	14

Table of contents(Cont)

Display uniformity	14
Field-of-view	15
Visual performance with the ANVIS	15
Resolution and ambient light level	15
Spatial contrast sensitivity and ambient light level	15
Temporal contrast sensitivity and ambient light level	16
Dynamic target identification	16
Field-of-view	16
Summary	17
New technology	20
New visual performance metrics	20
References	21

List of figures

1. Drawing of the IHADS with HDU and visor in place	6
2. IHADSS Combiner lens transmittance measured as a function of wavelength	7
3. IHADSS field curvature plotted as a function of change in focus with 8 different degrees of rotation	8
4. IHADSS spherical error plotted as a function of decentration	8
5. Spatiotemporal response of the IHADSS	10
6. Drawing of ANVIS attached to the SPH-4 helmet	12
7. Percent ANVIS distortion measured as a function of angular position	13
8. ANVIS output luminance as a function of night sky condition	14
9. Visual acuity with ANVIS as a function of night sky condition for targets of high and medium contrast	15
10. Spatial contrast sensitivity as a function of spatial frequency for different night sky conditions ..	16
11. Visual flicker sensitivity viewing alphanumeric characters through the ANVIS	17

List of tables

1. Summary table of IHADSS performance	18
2. Summary table of ANVIS performance	19

INTRODUCTION

The U.S. Army currently fields two helmet mounted display systems. These are the Integrated Helmet and Display Sighting System (IHADSS), which is employed on the AH-64 Apache, and the Aviator's Night Vision Imaging System (ANVIS), which is employed on all U.S. Army rotary wing aircraft, including the AH-64. The IHADSS has been fielded since 1985 and ANVIS came into general use during the latter 1980's. The ANVIS is based on third generation image intensification tubes; systems based on second generation image intensification tubes preceded ANVIS and were fielded as early as 1971.

The performance and figures-of-merit specifications of the IHADSS and the ANVIS provide a basis for judging performance of future aviation electro-optical devices. The ANVIS and IHADSS are fielded and proven systems which form a tangible basis for developing future designs and performance requirements. Future helmet mounted display designs must be required to provide performance which meets or exceeds the performance of currently fielded systems. This paper specifies in summary form performance parameters for different figures-of-merit which Jeanbe used to define the overall performance of the IHADSS and ANVIS. These values were obtained from an exhaustive literature search of test and evaluation data available on IHADSS and ANVIS. These values are intended to be used as a baseline for comparison of new systems. System parameters for which insufficient performance data are available also are noted. Most of the data specified in this paper is the result of physical and performance assessments performed at the U.S. Army Aeromedical Research Laboratory, Fort Rucker, Alabama (Rash et al., 1987; Kotulak, 1993; Rabin, 1994; Martin et al., 1994; Harding et al., 1995).

IHADSS SPECIFICATIONS

The IHADSS consists of various electronic components and a helmet/display system, called the Integrated Helmet Unit (IHU). The IHU includes a helmet, visor housings with visors, miniature cathode-ray-tube (CRT), and helmet display unit (HDU) [Figure 1]. The HDU serves as an optical relay device which conveys the image formed on the CRT through a series of lenses, off-axis beam splitter (often called a combiner), and into the aviator's right eye. The combiner is a multilayered dichroic filter which is maximized for reflectance at the peak emission of the P-43 phosphor. The IHADSS operates in conjunction with two forward looking infrared (FLIR) sensors located on the nose of the aircraft. One sensor, called the Pilot's Night Vision System (PNVS), provides pilotage imagery, while the second sensor, the Target Acquisition and Designation System (TADS), provides targeting imagery. Infrared detectors, mounted on the IHU helmet, allow the FLIR sensor to be slaved to the pilot's head movements. Aircraft parameters symbology, along with the imagery from the FLIR sensor, is presented to the pilot by means of the HDU. The HDU is designed so that the image of the 30-degree vertically by 40-degree horizontal field-of-view (FOV) of the sensors subtends a 30-by-40-degree field at the pilot's eye. The IHADSS is a monocular display, presenting imagery to the right eye only. At night and under inclement weather conditions, the HDU imagery may be the sole source of information by which the

pilot flies the aircraft. The visual quality of this imagery is of supreme importance.

Performance specifications for the IHADSS have been divided into two categories: optical and electro-optical. Optical specifications deal with the propagation of the relay and see-through optics. Electro-optical specifications deal with the image as generated by the CRT. Most of the physical measurements that specify the performance of the IHADSS are found in USAARL Laboratory Report 95-32 (Harding, Beasley, Martin and Rash 1995). We also included limited discussion on visual performance with the IHADSS.

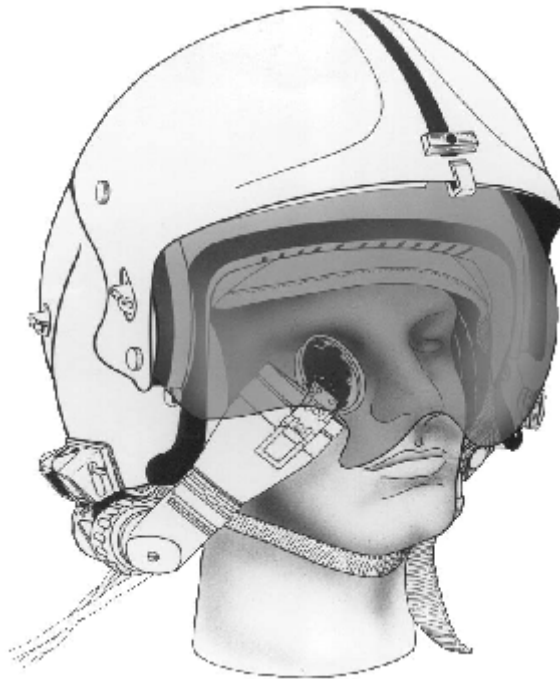


Figure 1. Drawing of the IHADSS IHU and visor in place.

IHADSS optical specifications

Combiner lens transmittance. Transmittance of light through the HDU combiner lens from the ambient scene is orientation dependent. We estimate that the plane of the combiner lens is approximately 23 degrees off parallel to the front surface of the eye. Harding et al., (1995) measured transmittance at different angles in 2-degree increments. Figure 2 shows the transmittance they measured at 22 degrees off normal. The dip in the transmittance curve allows greater reflectance of the output of the IHADSS tube and therefore greater IHADSS luminance reaches the eye. The average transmittance between 400 and 700 nanometers (nm) is 36 percent.

Distortion. IHADSS distortion was measured using an Ann Arbor optical tester, the image of a Ronchi ruling was viewed after having passed through the optics of the HDU combiner lens twice. Comparing the imaged ruling to standards in MIL-V-43511C revealed nonsignificant levels of distortion. A value of less than 1 was assigned the distortion image.

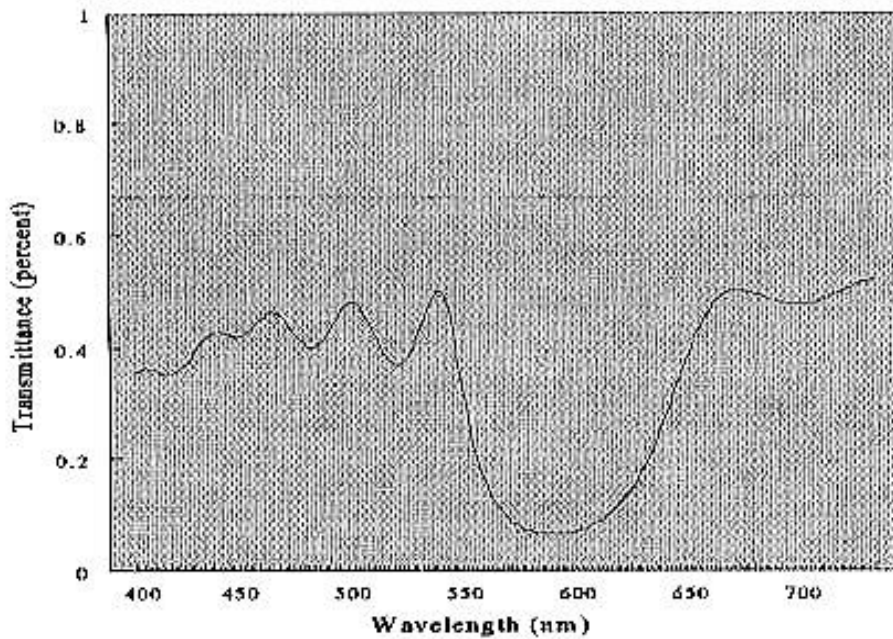


Figure 2. IHADSS combiner lens transmittance measured as a function of wavelength. The combiner lens was set to an angle 22 degrees off normal. From Harding et al., 1995.

Optical aberrations. Field curvature and spherical aberration were measured using a dioptometer to measure errors in focus with changes in orientation (field curvature) or changes in decentration (spherical aberration). In Figure 3, field curvature data is plotted as a function of change in focus with changes in rotation (orientation). The difference between the vertical and horizontal focuses at each degree of rotation is a measure of astigmatic error.

In Figure 4, spherical aberration is plotted as a function of decentration. The amount of decentration is limited by the size of the exit pupil. Since the size of the exit pupil was approximately 10.5 mm, the measurement at 6 mm shown in the figure is suspect. The data are an average of the values obtained bilaterally out to 5 mm.

Magnification. HDU generated images show little or no deviation from unity magnification. The sensor to display fields-of-view aspect ratio and magnification are maintained.

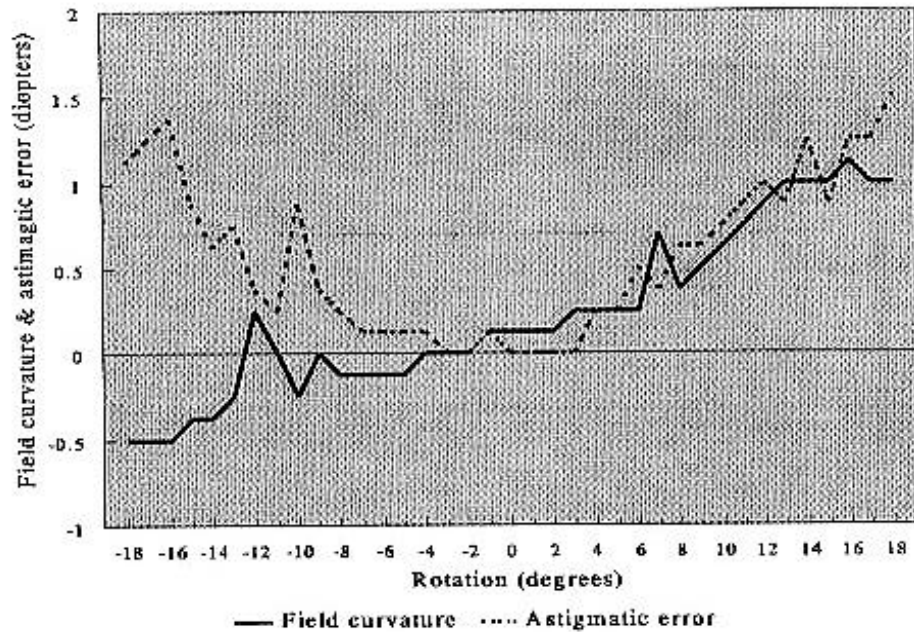


Figure 3. Field curvature plotted as a function of change in focus with different degrees of rotation. The astigmatic error represents the magnitude separation in diopters between the vertical and horizontal focus. From Harding et al., 1995.

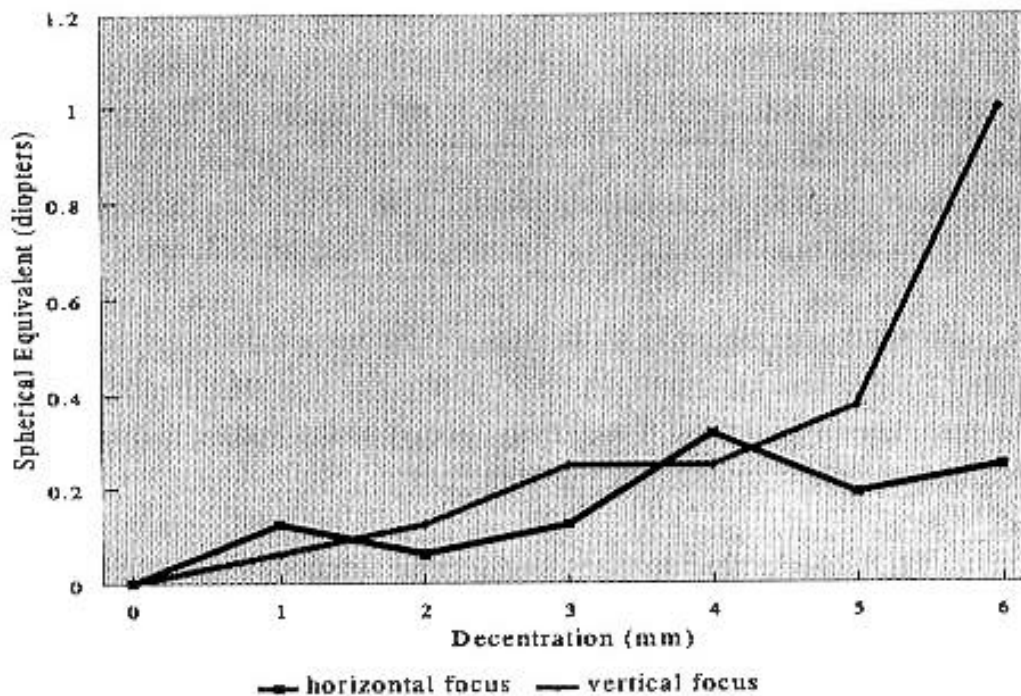


Figure 4. Spherical error plotted as a function of decentration. The separation between the two curves is a measure of astigmatic error. From Harding et al., 1995.

Field-of-view. IHADSS field-of-view was measured by filling the CRT with a uniform light pattern and then measuring luminance output as a function of IHADSS rotation. Harding et al., (1995) measured the horizontal and vertical fields of view of the displayed IHADSS image to be approximately 40 and 31 degrees, respectively.

Eye relief Optical eye relief is defined as the distance along the optical axis from the last optical element (e.g., IHADSS HDU combiner lens) to the exit pupil. Perhaps of more functional importance is the notion of 'physical eye relief' which is defined as the distance from the closest display system component to the exit pupil. Physical eye relief determines system compatibility with auxiliary devices, e.g., corrective lenses, protective masks, etc. Harding et al., (1995) measured optical and physical eye relief under two different conditions. The conditions were with the combiner lens (a) fully retracted, and (b) fully extended. These two conditions represent the far and near extremes of eye relief. Under condition 'a', optical eye relief equaled 40.12 mm and physical eye relief equaled 13.18 mm. Under condition 'b', optical eye relief equaled 25.76 mm and physical eye relief equaled a - 5.99 mm. The negative physical eye relief in condition 'b' underscores the potential problem associated with relying upon optical eye relief measurements.

Exit pupil (size and shape). The size of the exit pupil was measured by focusing on the exit pupil with a short working distance telescope which was mounted to a precision stage. When viewed through the telescope, the exit pupil appeared as a circular patch of light. Harding et al., (1995) measured the horizontal and vertical extent of the patch of light using the precision stage which had an incremental accuracy of just a few microns. The horizontal and vertical diameters were virtually identical thus providing a circular diameter of 10.57 mm.

Focus adjustment range. There is a focus adjustment on the barrel of the IHADSS HDU which allows the user to bring the imagery into sharp focus. Harding et al., (1995) measured this range to be - 6.250 to +3.625 diopters.

IHADSS electro-optical specifications

Dynamic luminance range. The luminance range of the miniature CRTs is rather high and is limited by spectral filtering, the HDU amplification circuits and the typical operational/user settings. By focusing at the exit pupil formed by the HDU, Harding et al., (1995) found a maximum luminance output of about 640 fL at saturation. This output was achieved by providing a 1 volt peak-to-peak NTSC signal to the CRT amplification circuits.

Dynamic modulation transfer function (MTF). The dynamic MTF of the HDU is defined by a spatiotemporal surface whose amplitude is modulation depth at each combination of spatial and temporal frequencies. From a visual standpoint, luminance contrast is of greater importance than modulation depth. Harding et al., (1995) measured a form of luminance contrast, termed Michaelson contrast, over a range of spatial and temporal frequencies. Figure 5 shows six spatial curves measured at six different temporal frequencies. Below 2 Hz, the curves are well grouped. Above

2
Hz
the
y
noti
ced
a
slig
ht
incr
ease
in
con
tras
t
whi
ch
is
aty
pic

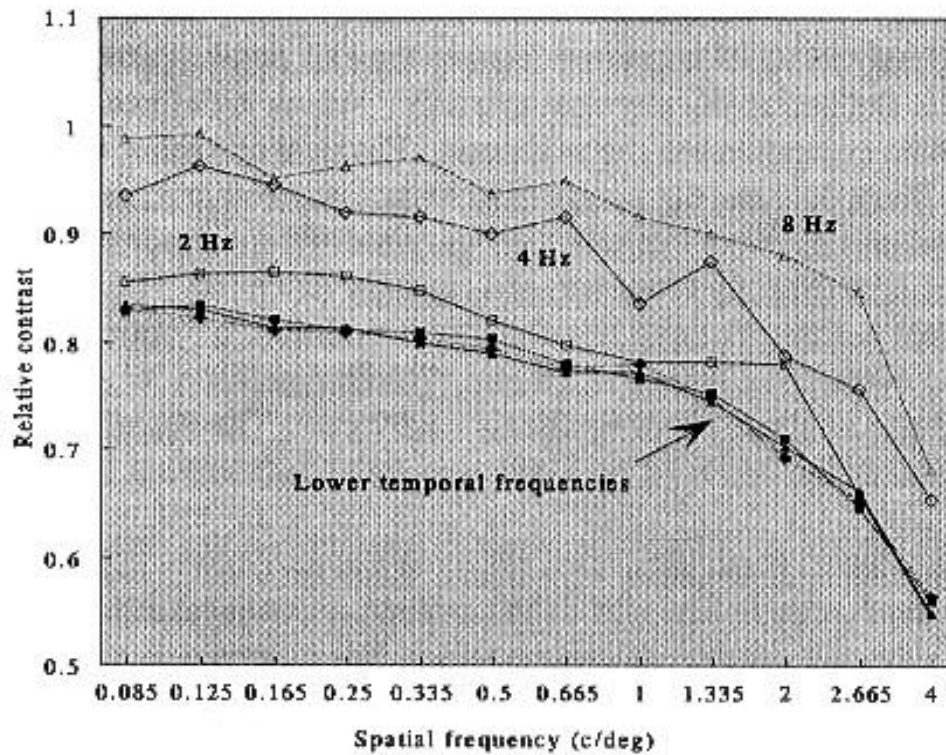


Figure 5. Spatiotemporal response of the IHADSS. Curves reflect, when appropriately scaled, the dynamic MTF of the system.

most CRT curves and must be due to the amplification circuits. The drive electronics for the IHADSS CRT must have a high temporal response.

Contrast ratios. By focusing a photometer through the exit pupil to the center of the HDU's field-of-view, Harding et al., (1995) measured contrast ratios under different luminance conditions. By setting the luminance and contrast to maximum, they found a contrast ratio at saturation to be about 3.0 (640/210). To define the contrast ratio over a more usable operational range, two levels were chosen (15 and 150 fL peak luminance) to correspond with lighting conditions encountered while flying with ANVIS and under daytime conditions. For setting the output, they set the contrast to zero and adjusted the peak brightness to 1 fL. They then adjusted contrast until they achieved a luminance of either 15 fL or 150 fL at the peak. Under these conditions, they found contrast ratios of 13.6 (15/1.1) and 33.3 (150/4.5), respectively.

Gray shades. By defining gray shade increments as multiples of $2^{(0.5)}$, the number of gray shades can be calculated from the contrast ratios specified above. For contrast ratios of 13.6 and 33.3, we found 8 and 11 gray levels, respectively.

Display chromaticity. The spectral output of the HDU with the P-43 phosphor is narrow banded with a peak transmittance at 544 nm. This peak corresponds with the peak of the P-43 phosphor. The width of the spectrum is about 4 to 6 nm at a level equal to 50 percent of the peak. The sidebands of the P-43 phosphor are filtered out by the HDU optical filter. Chromaticity coordinates for the spectrum are $x=0.2774$, $y=0.7089$ and $u'=0.1013$, $v'=0.5826$ for the 1931 and 1976 CIE coordinates, respectively.

Display uniformity. Display/luminance uniformity was measured in the vertical and horizontal meridian of the field-of-view. The luminance fell off abruptly at the extremes of the field-of-view. Independent values were obtained for each meridian by measuring luminance uniformity to within one degree of the field-of-view border. The vertical mean luminance was 129 ± 13.2 fL and the horizontal mean luminance was 124 ± 19.6 fL. The larger horizontal standard deviation is due to the greater luminance fall-off in the peripheral field-of-view.

Visual Performance with the IHADSS

Actual IHADSS performance may vary greatly from the performance measurements presented above depending upon aviator settings, head and face anthropometry, and HDU/combiner lens adjustments. The performance metrics mostly affected by the user are luminance, contrast ratios and field-of-view.

Visual resolution. Visual resolution and contrast of IHADSS imagery are dependent on ambient light levels, background luminance and texture, and control settings of display contrast and brightness, and PNVIS sensor settings of gain and bias level (Rash et al., 1990). Rash and Behar (1990) showed 90 percent of Apache aviators misadjusted the HDU focus setting by a mean of -2.25 diopters. Even without this potential problem, Snellen visual acuity with the Apache PNVIS/IHADSS system is cited as 20/60 (Greene, 1988).

Field-of-view. A very important lesson learned during the early fielding of the IHADSS was the impact of fitting on the ability of the aviator to achieve the full 30- x 40-degree field-of-view (Rash et al., 1987). Unless considerable care is taken in fitting of the IHADSS IHU and HDU to the user, with special concern paid to head and face anthropometry and final extension of the combiner, a serious loss of field-of-view can occur. In addition, the integration of chemical protective masks with the IHADSS can cause similar losses in achievable field-of-views (Rash and Martin, 1987).

ANVIS SPECIFICATIONS

The ANVIS is a binocular helmet mounted display based on third generation image intensification tubes (Figure 6). These tubes use the principle of photomultiplication to amplify low level ambient light. ANVIS is sensitive to spectral energy between 550 to 950 nanometers. Photons falling on a photocathode produce electrons which are multiplied within a microchannel plate and then strike a phosphor screen, producing an amplified image of the outside scene (Verona and Rash, 1989). The ANVIS currently uses a P-22 phosphor but is planned to be changed to the faster P-43 phosphor. The spectral output of the ANVIS which reaches the eye corresponds to the phosphor's spectrum, not to the spectrum of the ambient scene.

Performance specifications for the ANVIS have been divided into two categories: optical and electro-optical. Optical specifications deal with the physical light conversion path and with user controls. Electro-optical specifications deal with the image as generated by the amplification tube, microchannel plate and phosphor display. We also include a discussion on visual performance with the ANVIS.

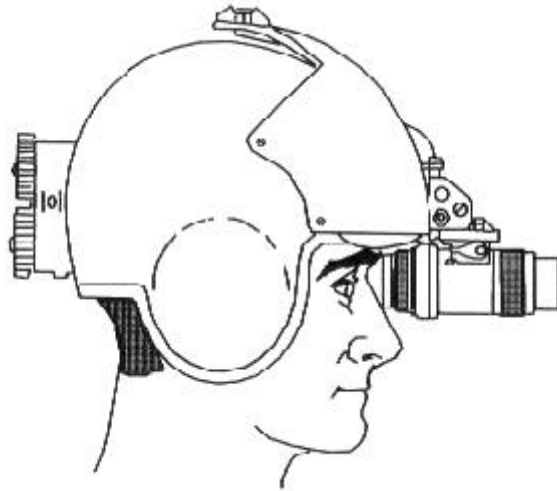


Figure 6. Drawing of ANVIS attached to the SPH-4 helmet. Attached to the rear of the helmet is the ANVIS battery pack which serves as a counterbalance.

ANVIS optical specifications

Distortion. Distortion in the ANVIS is best described by a curve which shows distortion in percent as a matter of angular position (Figure 7). As can be seen, little distortion is apparent even at extreme angular positions. MIL-A-49425 (CR) states that distortion shall be no greater than 4 percent across the field-of-view. Martin et al., (1994) found distortion values less than 2 percent.

Magnification. Sighting through the ANVIS should have unity gain and any deviation from this would be an estimate of magnification. Measurements taken by Martin et al., (1994) using a precision test method, found a magnification of 2 percent or less. MIL-A-49425 (CR) states that magnification shall be less than ± 5 percent.

Eye relief. Physical eye relief distance for the ANVIS can be specified as the greatest vertex distance where the entire 40-degree field-of-view is still visible. The distance from the anterior surface of the cornea to the surface of the last lens element of the ANVIS is specified as the vertex distance. Beyond a vertex distance of 20 mm, the field-of-view is proportionately reduced (Kotulak, 1992; McLean, 1995). Thus, 20 mm is a good estimate of eye relief.

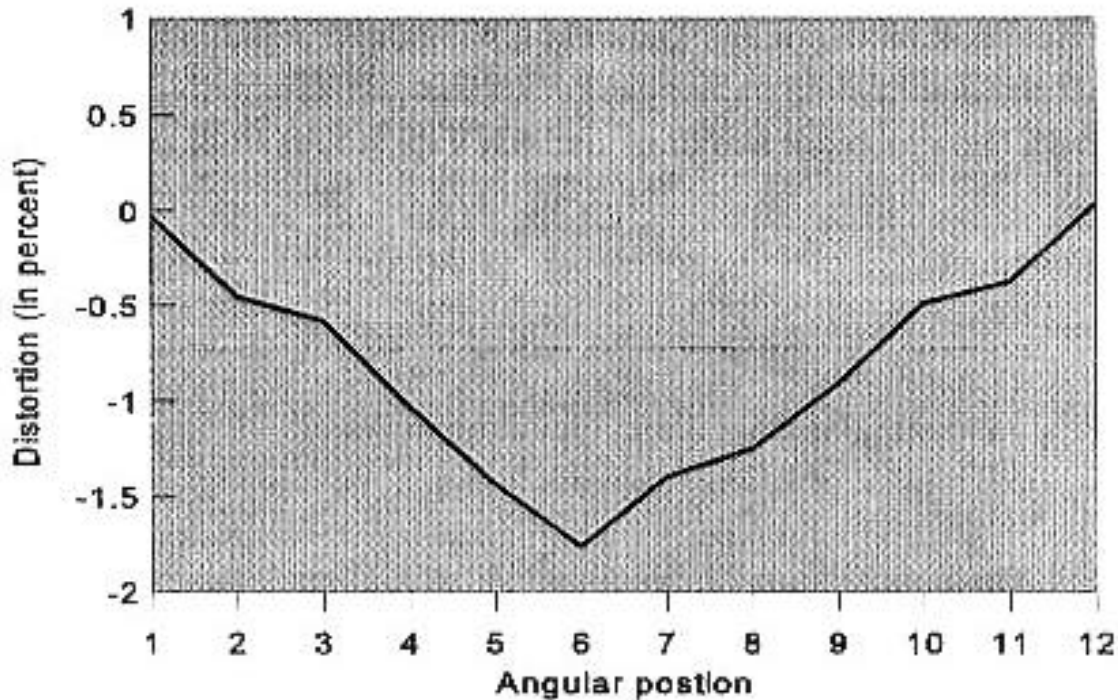


Figure 7. Percent ANVIS distortion as a function of angular position. Data taken from Martin et al., (1994).

Exit pupil. The ANVIS does not form an exit pupil per se at the eye, however, an effective exit pupil size can be defined at any specified vertex distance within the cone defined by the marginal rays.

Focus adjustment range. In MIL-A-449425 (CR), the objective focus range is specified as 28 ± 3 cm to infinity. The eyepiece focus range is +2 to -6 diopters.

Interpupillary adjustment. The specifications (MIL-A-49425 (CR)) for the interpupillary adjustment range are 52 to 72 mm.

Collimation. Collimation in the sense of the ANVIS is not a measurement of parallel light rays but rather is a measurement of the alignment between the left and right optics of the ANVIS. The divergence/convergence between the light beams emitted from the two eyepieces is less than 1 degree.

ANVIS electro-optical specifications

Dynamic luminance range. ANVIS display luminance is a function of target and ambient light levels. Rabin (1994) evaluated ANVIS output luminance as a function of steady ambient light levels. The light levels emulated night sky conditions. Figure 8 shows a plot of ANVIS output luminance as a function of night sky condition. Through a calibration procedure, Rabin found an approximate three log

unit dynamic range for the ANVIS, although under typical night sky conditions (Figure 8), the dynamic range of the ANVIS is less than two log units.

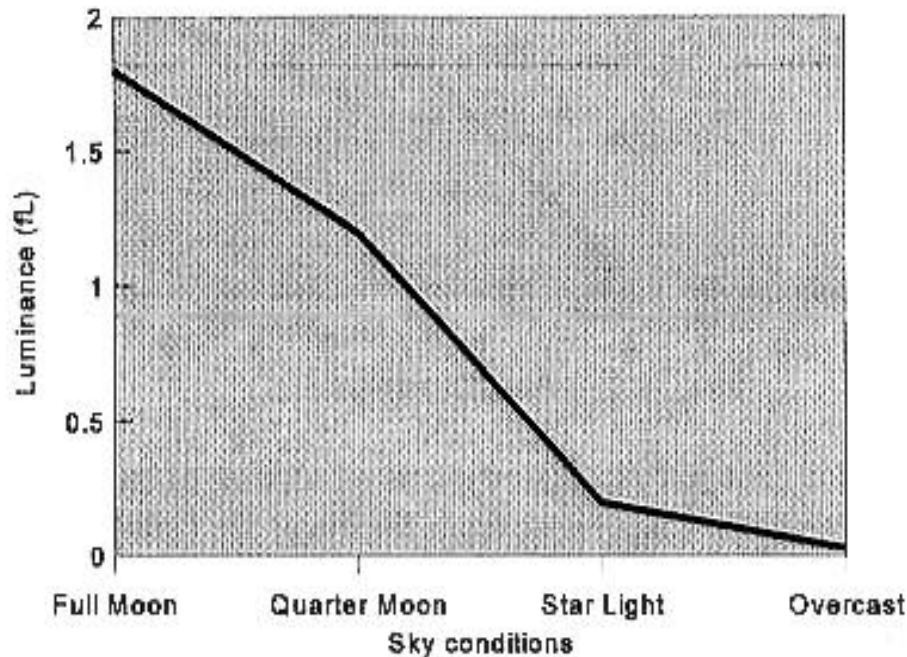


Figure 8. ANVIS output luminance as a function of night sky condition. Data from Rabin, 1994.

Dynamic MTF. The dynamic MTF of the ANVIS has not been done due to the difficulty in generating mathematically precise near infrared images.

Contrast ratio. Target contrast is dependent upon target size, target reflectance, and lighting conditions. The luminance output of the ANVIS is linear to the point of saturation. For a small high contrast target, ANVIS contrast is high. According to unpublished data by W.E. McLean, contrast ratios of 33 (peak luminance/background luminance) are easily obtained. For small point sources of light, such as ground vehicle lights seen from afar, much higher contrast ratios are achievable.

Gray shades/levels. For a contrast of 33, 11 gray shades are available based upon a one-half octave increment between levels.

Gain. The light amplification gain of the ANVIS is dependent upon the automatic gain control mechanism. For extremely low luminance levels, a gain of 3000 is possible.

Display chromaticity. The ANVIS output using the P-22 phosphor is broadband with the peak wavelength at 537 nm. The chromaticity coordinates are $x=0.3143$, $y=0.5983$ and $u'=0.1316$, $v'=0.5639$ for the 1931 and 1976 CIE coordinate systems, respectively.

Display uniformity. Display uniformity has not been measured for the ANVIS.

Field-of-view. Field-of-view was measured by Martin et al., (1994) and was found to be 40.4 degrees. The technique they used measured the light output of the ANVIS as a function of angular rotation. Extreme light fall-off at the borders of the field-of-view made the field-of-view measurements reliable.

Visual performance with the ANVIS

Resolution and ambient light level. Visual acuity with the ANVIS is dependent upon ambient light level and target contrast. In general, the higher the contrast and higher the ambient light level the higher the acuity. Figure 9 shows Snellen acuity as a function of night sky conditions. For high contrast targets, Snellen acuity is better than 20/40 under full moon lighting conditions and falls off gradually to about 20/80 under overcast starlight conditions. For medium contrast targets, Snellen acuity is about 20/50 under full moon conditions and falls to about 20/300 under overcast starlight conditions.

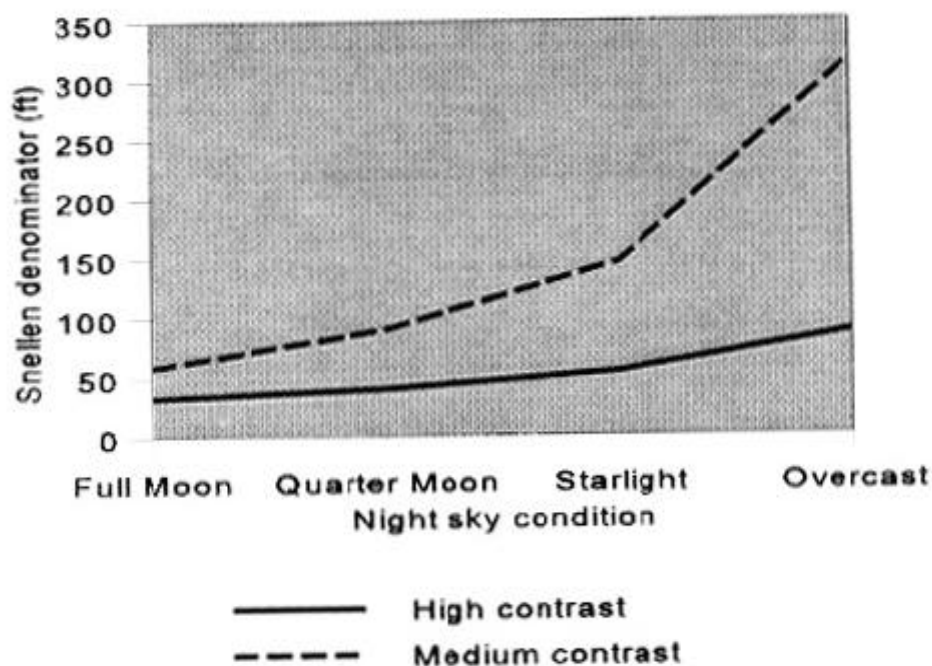


Figure 9. Visual acuity with ANVIS as a function of night sky condition for targets of high and medium contrast. Data from Kotulak and Rash, 1992.

Spatial contrast sensitivity and ambient light level. Like visual acuity, spatial contrast sensitivity is likewise affected by ambient light levels. The lower the light level, the lower the contrast sensitivity. Figure 10 shows spatial contrast sensitivity as a function of four ambient light levels. Note the fall-off in sensitivity with increased spatial frequency.

Temporal contrast sensitivity and ambient light level. True temporal contrast sensitivity has not been measured using ANVIS. What has been measured is flicker sensitivity to an on-off target (Rabin, 1944). The target was a set of seven flickering letter 'Es' each measuring 75 minutes of arc but having different contrasts. The contrasts ranged from 4 to 100 percent in 0.23 log unit increments. The task was to identify the flickering 'E'. Figure 11 shows flicker sensitivity to four night sky conditions. Notice that flicker

greatest
moon
and falls
ambient
conditions
reduced.

sensitivity is
under full
conditions
off as the
sky lighting
are

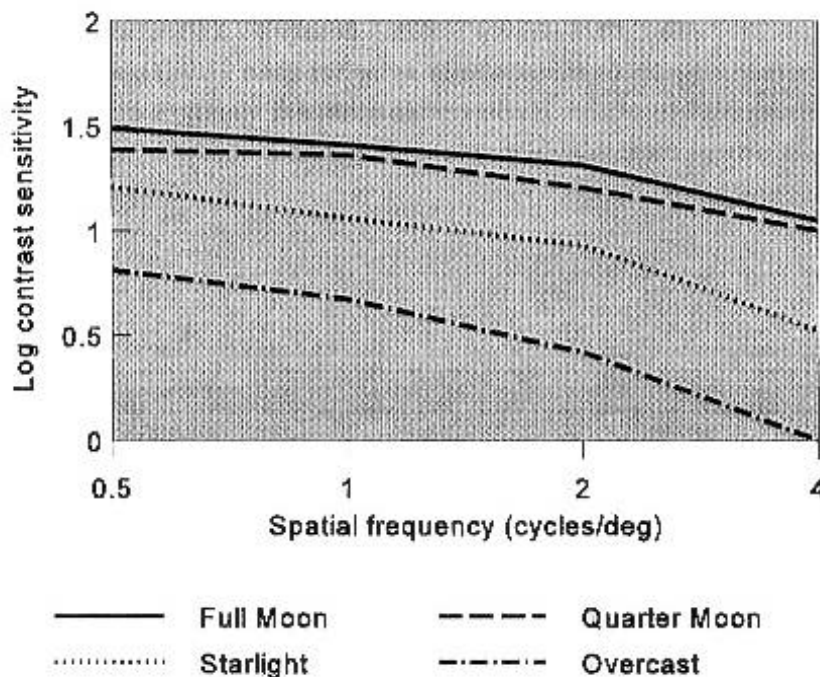


Figure 10. Spatial contrast sensitivity as a function of spatial frequency for different night sky conditions. Data from Rabin, 1994.

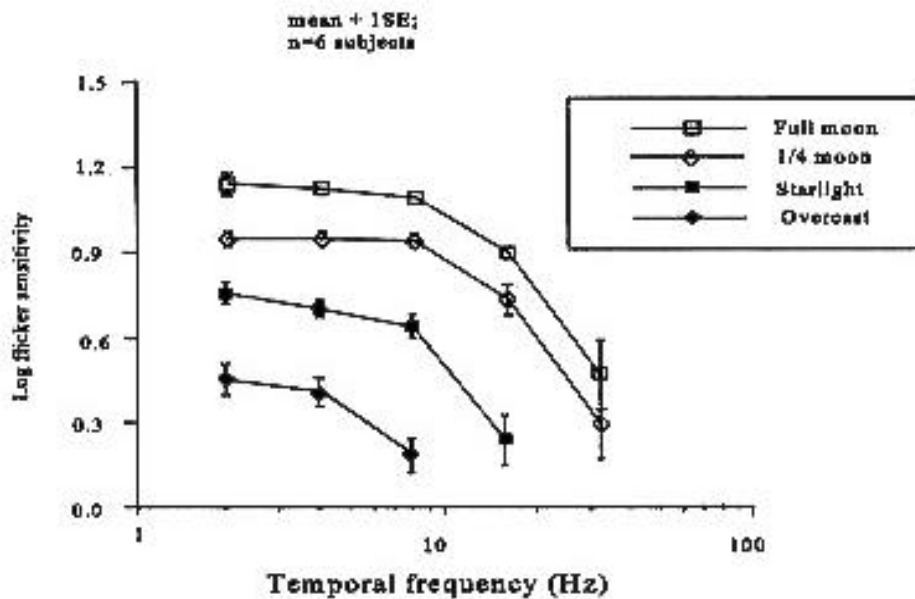


Figure 11. Visual flicker sensitivity viewing alphanumeric characters through the ANVIS. Data from Rabin (1994).

Dynamic target identification. There is no standard psychophysical procedure for specifying target identification performance.

Field-of-view. Field-of-view is dependent upon the distance from the eye to the anterior portion of the last lens element of the ANVIS (sometimes referred to as the vertex distance) (Kotulak, 1992). Within the eye relief distance the field-of-view is around 40 degrees. With vertex distances greater than 20 mm, the field-of-view decreases proportionally to the increase in distance. At 50 mm vertex distance, the field-of-view has fallen to 25 degrees.

SUMMARY

These data presented are a compendium of general performance specifiers for fielded army helmet mounted display systems. The data were taken from published and unpublished reports and represent a summary description of these electro-optical systems. The IHADSS and ANVIS data are summarized in Tables 1 and 2, respectively. Comparisons between these two systems are not warranted since the systems are based on different operating principles.

Table 1.

Summary table of IHADSS performance

Test parameter	Performance measurement/specification
Optical	
Combiner lens transmittance	36 percent between 400 and 700 nm
Distortion	<1 by MIL-V-43511C scale
Optical aberrations	See Figures 3 and 4.
Magnification	Unity
Field-of-view	40 degrees horizontal x 31 degrees vertical
Eye relief	Combiner fully retracted: Optical eye relief of 40.12 mm Physical eye relief of 13.18 mm Combiner fully extended: Optical eye relief of 25.76 mm Physical eye relief of -5.99 mm
Exit pupil	Circular, diameter of 10.57 mm
Focus adjustment range	-6.250 to +3.625 diopters
Electro-optical	
Dynamic luminance range	640 fL peak
Dynamic MTF	See Figure 5.
Contrast ratios	13.6 for 15 fL peak luminance 33.3 for 150 fL peak luminance
Gray shades	8 for 15 fL peak luminance 11 for 150 fL peak luminance
Display chromaticity	$x=0.2774$, $y=0.7089$ and $u'=0.1013$, $v'=0.5826$
Display uniformity	Vertical: 129 ± 13.2 fL Horizontal: 124 ± 19.6 fL

Table 2.

Summary table of ANVIS performance

Test parameter	Performance measurement/specification
Optical	
Distortion	Less than 2 percent
Magnification	Less than 2 percent
Eye Relief	20 mm or less
Exit pupil	effective exit pupil defined by vertex distance
Focus adjustment and range	range 28 ± 3 cm to infinity adjustment: +2 to -6 diopters
Electro-optical	
Dynamic luminance range	See Figure 8.
Dynamic MTF	Data not available
Gray shades	11 gray shades for naturally illuminated objects
Contrast ratios	33 to 1 for naturally illuminated objects
Gain	3000X
Display chromaticity	$x=0.3143$, $y=0.75983$ and $u'=0.1316$, $v'=0.5639$
Display uniformity	Data not available
Field-of-view	40.4 degrees circular

NEWER TECHNOLOGY

This last decade has seen widespread advances in flat panel technology spurred in large part by the ever increased market share of portable computers with the market desiring faster displays with greater spatial and color resolution, and by the portable television market and by other related markets. The consumer has seen the advantage of flat panel technology and the manufacturers have escalated their capital investment into the development of new and better displays and manufacturing processes. Fully capitalizing on this growth industry and with the wish to develop an industrial base, the Department of Defense has funded an initiative to provide American firms R&D dollars to develop flat panel technologies. With manufacturers striving for increased miniaturization and greater resolution, the flat panel displays are now competing with other technologies for operational consideration. Flat panel technology provides the aviation community with an alternative electro-optical display that is lighter in weight, lower in cost, lower in power consumption and smaller in size. Prototype helmet mounted displays are being developed which use miniature high definition flat panel technology for image generation. The new technology is also being used in designs and prototypes for the next generation night vision devices as symbolology generators. Cockpit displays are already being produced using the new technology.

NEWER VISUAL PERFORMANCE METRICS

The image quality of electro-optical display information must be assessed in terms of viewing conditions (e.g., visual distance from eye to display, display size, display luminance and lighting conditions) and in terms of operational figures-of-merit. Image quality of an electro-optical display information must be defined in terms that are directly relatable to human visual performance. Further, image quality metrics must include measures relatable to ease of human target detection and recognition. Progress has been made in relating electro-optical display characteristics to a human factors assessment. Early in the history of display ergonomics, the metric MTF_A (Charman & Olin, 1965) provided a measure that had some success in predicting image quality. The MTF_A however over-simplified visual task performance and violated certain mathematical principles. Because of this oversimplification, other metrics have been developed. Of recent significance is the work of Peter Barten (1990, 1993) and the "Square-root integral" assessment method (SQRI).

The SQRI is given by

$$SQRI = \int_0^{\infty} \frac{M(u)}{M_t(u)} du$$

where $M(u)$ is the MTF of the display and $M_t(u)$ is the visual contrast threshold curve, and u is spatial frequency per unit angle at the eye of the observer. The integration extends over the range from 0 to maximum spatial frequency. This equation thus takes into consideration the spatial frequency description of the display and the visual system. Good agreement has been found between the SQRI and subjective measures of image quality (Barten, 1990, 1993; Westerink & Roufs, 1989).

Scientists from Honeywell, Inc. (Nelson and Cox, 1992) have developed a model for

assessing HMD designs based upon a linear systems approach. The approach calculates the frequency transfer characteristics of each major component in an HMD design and feeds that information into a simplified spatial model of human visual perception. The model, although well done, neglects the important temporal characteristics of the HMD and vision.

A metric similar to the SQRI and the Honeywell model but incorporating temporal characteristics must be developed for head mounted displays so as to streamline human factors assessment and to improve system acceptance.

Image quality must also reflect what types of information the electro-optical display is intended to present. For example, if only alphanumeric characters will be presented, the low spatial frequency range of the display is of less importance than the high spatial frequency range. To reflect this relationship between spatial frequency bands and performance, new human factor metrics must be developed to relate subjective image quality to electro-optical display figures of merit.

Future cockpit electro-optical designs would benefit from a well crafted human factors assessment technique which is patterned after the SQRI metric.

REFERENCES

- Behar, I. and Rash, C. E. 1990. Diopter focus adjustment of Apache IHADSS. *Aviation Digest*, 1-90-1:14-15.
- Barten, P.G.J. 1990. Evaluation of subjective image quality with the square-root integral method. *J. Opt. Soc. Am. A*, 7:2024-2031.
- Batten, P.G.J. 1993. Effects of quantization and pixel structure on the image quality of color matrix displays. *J. SID*, 1:147-153.
- Charman, W.N. and Olin A. 1965. Tutorial: image quality criteria for aerial camera systems. *Photographic Science and Engineering*, 9:385-397.
- Greene, D.A. 1988. Night vision pilotage system field-of-view (FOV)/resolution tradeoff study flight experiment report. Fort Belvoir, VA: U.S. Army Night Vision Laboratory. NV 1-26.
- Harding, T.H., Beasley, H.H., Martin, J.S., and Rash, C.E. 1995. Physical evaluation of the integrated helmet and display sighting system (IHADSS) helmet display unit (HDU). Fort Rucker, AL: U.S. Army Aeromedical Research Laboratory. USAARL Report No. 95-32.

Kotulak, J.C. 1993. In-flight field-of-view with ANVIS. Fort Rucker, AL: U.S. Army Aeromedical Research Laboratory. USAARL Report No. 93-8.

Martin, J.S., Beasley, H.H., Verona, R.W. and Rash, C.E. 1994. Semiautomated methodology for measurement of field-of-view, and distortion of night vision devices as defined in MIL-A-49425(CR). Fort Rucker, AL: U.S. Army Aeromedical Research Laboratory. USAARL Report No. 94-25.

McLean, W.E. 1995. Video method of measuring field-of-view of electro-optical devices versus eye clearance. Fort Rucker, AL: U.S. Army Aeromedical Research Laboratory. USAARL Report No. 95-30.

Rabin, J. 1994. Spatial contrast sensitivity through aviator's night vision imaging system (Reprint). Fort Rucker, AL: U.S. Army Aeromedical Research Laboratory. USAARL Report No. 94-19.

Rash, C. E. and Martin, J. S. 1987. The Effect of the M-43 Chemical Protective Mask on the Field-of-View of the Helmet Display Unit of the Integrated Helmet and Display Sighting System. Fort Rucker, AL: U.S. Army Aeromedical Research Laboratory. USAARL LR 87-10-2-5.

Rash, C. E., Martin, J. S., Gower, D. W., Licina, J. R., and Barson, J.V. 1987. Evaluation of the U.S. Army Fitting Program for the Integrated Helmet Unit of the Integrated Helmet and Display Sighting System. Fort Rucker, AL: U.S. Army Aeromedical Research Laboratory. USAARL Report No. 87-8.

Rash, C. E., Verona, R. W., and Crowley, J. S. 1990. Human factors and safety considerations of night vision systems flight using thermal imaging systems, Helmet-Mounted Displays II. R. J. Lewandowski, Editor. Proceedings SPIE. 1290:142-160.

Nelson, S.A. and Cox, J.A. 1992. Quantitative helmet mounted display system image quality model. Helmet-Mounted Displays II. R. J. Lewandowski, Editor. Proceedings SPIE. 1695:128-137.

Westerink, J.H.D.M. and Roufs, J.A.J. 1989. Subjective image quality as a function of viewing distance, resolution, and picture size. *SMPTJ*, 98:113-119.